Synthetic Thermosphere Winds based on CHAMP neutral and electron densities

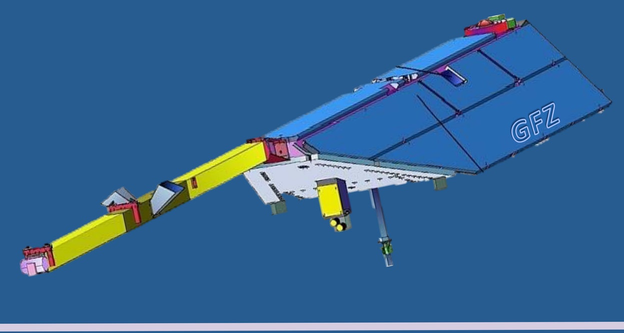

F. Gasperini[1] (gasperini@colorado.edu), J. M. Forbes[1], E. N. Doornbos[2], and S. L. Bruinsma[3]

(1) University of Colorado, Boulder, CO, USA, (2) Delft University of Technology, Delft, The Netherlands, (3) National Center for Space Studies (CNES), Toulouse, France

Introduction

- Zonal winds are responsible for the generation of electric fields via the *F* region dynamo mechanism, while meridional winds modify the ionosphere by moving plasma up and down magnetic field lines. Knowledge of meridional winds is key to understanding latitudinal and thermosphere-ionosphere coupling, and yet global measurements of this wind component are scarce.
- In the 60's and 70's thermosphere winds were obtained solving the momentum equations with crude models of pressure gradient and ion drag (*Challinor, 1969; Geisler, 1966*).
- Here we present a **new method to estimate zonal and meridional thermospheric neutral winds (*synthetic winds*)** for solar low and geomagnetic quite conditions using data from the Challenging Minisatellite Payload (CHAMP) satellite.

Data and Methodology

- CHAMP was lunched in 2000 in an almost circular, near-polar, slowly precessing orbit, and provided homogeneous and global coverage until 2010.
- Neutral density and zonal (cross-track) wind from CHAMP accelerometer [*Bruinsma et al.*, 2004; *Doornbos et al.*, 2010], and electron density from CHAMP Langmuir probe [*Cooke et al.*, 2003] are used.
- To derive thermosphere neutral winds the following 3-step procedure is adopted:

Step 1: *Deriving temperature and ion drag from neutral and electron density.*

i. Starting from CHAMP total mass densities (ρ) we use the NRLMSISE00 empirical model and iterate on F10.7 until the model density converges on the measured density (±1%), yielding the equivalent model exosphere temperature (T).

ii. Ion drag coefficients (λ) are inferred from CHAMP electron density.

Step 2: *Deriving pressure gradients from neutral density and temperature.*

i. Pressure (p) is inferred from neutral density and temperature using the ideal gas law ($p=\rho R_{spec}T$).

ii. Eastward (PGX) and northward (PGY) pressure gradients are derived by calculating derivatives with respect to longitude (φ) and latitude (ϑ)

$$PGX = \frac{1}{R_E\,\rho\cos\theta}\frac{\partial p}{\partial \phi}\;;\quad PGY = \frac{1}{R_E\,\rho}\frac{\partial p}{\partial \theta}$$

and R_E=Earth's radius.

Step 3: *Solving the 2-D momentum equations for the horizontal wind field.*

i. Neglecting vertical viscosity, plasma drifts, parallel ion drag, horizontal/vertical advection, and momentum force, we solve for the zonal (u) and meridional (V) wind

$$\frac{\partial u}{\partial t} = 2\Omega v\sin\vartheta - \lambda u - PGX\;;\quad \frac{\partial v}{\partial t} = 2\Omega u\sin\vartheta - \lambda v\sin^2 I - PGY$$

where t=UT-time, Ω=Earth's rotation rate, I=dip angle.

Local Time Reconstruction & Results

Local Time Reconstruction

- We selected 7 solar low and geomagnetic quite 10-day periods within the 43-day period 1 Aug-12 Sept spanning the years 2007-2009 (*Tab 1*).

Local Time	10-day Period	F10.7
03 – 15	30/08/07-09/09/07	69
04 – 16	20/08/07-29/08/07	71
10 – 22	04/08/09-13/08/09	68
17 – 05	03/09/08-12/09/08	67
18 – 06	24/08/08-02/09/08	67
19 – 07	12/08/08-22/08/08	67
20 – 08	01/08/09-11/08/08	67

Table 1. *Local time and average solar flux level for each of the seven 10-day periods selected for the local time reconstruction.*

- We least square fit all the waves and refer to this 43-day period, for which all latitudes, longitudes, and local times are sampled, as an ***equivalent day***.
- Averaging only 43 days, instead the 130 days needed for CHAMP to cover all local times, reduces the effect of amplitude suppression due to averaging and mixing of seasons.
- Strong correlation (r=0.81) is found between synthetic zonal winds and cross-track winds for the seven 10-day periods (*Fig 1*).
- We estimated that the ***synthetic zonal and cross-track winds share over 65% of the variance*** in latitude-longitude structures, with no detectable bias.

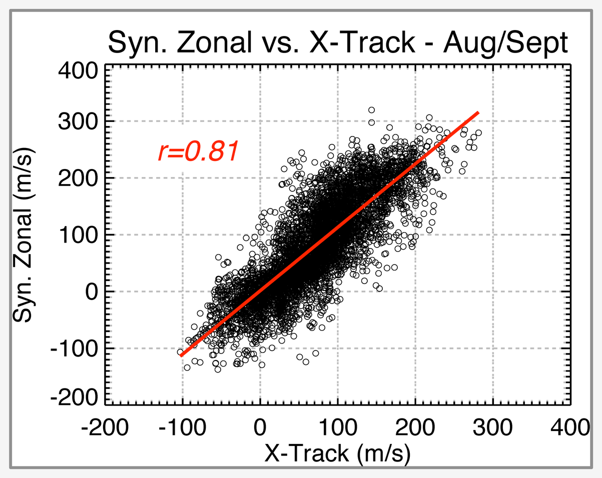

Figure 1. *Scatter plot between synthetic zonal and cross-track winds for the seven 10-day periods in Tab 1.*

Latitude vs. Local Time

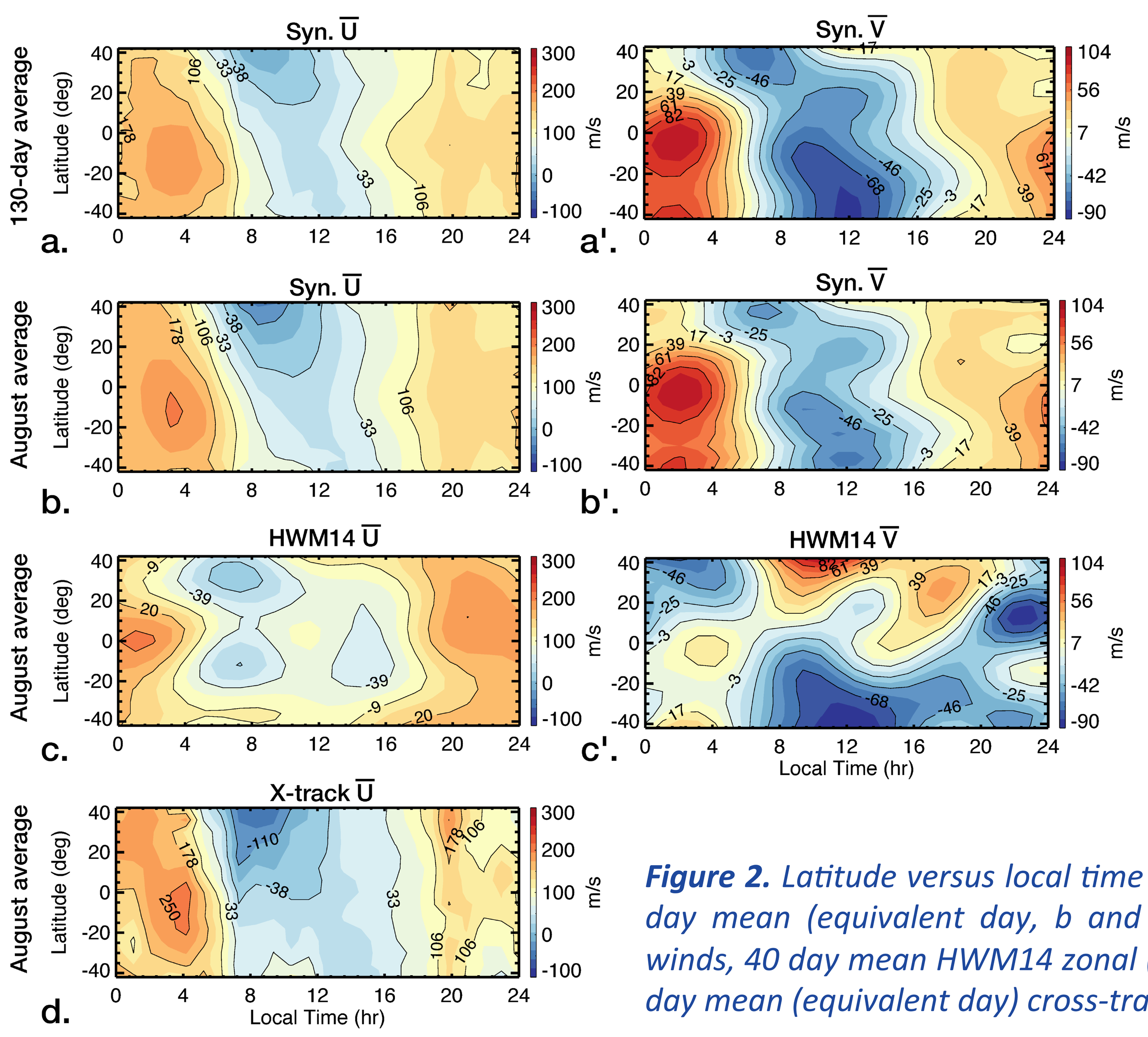

- HWM-14 fails to reproduce most of the observed local time and latitude variability in the winds (*Fig 2*).
- Averaging 130 days of data leads to amplitude suppression by up to 30%, compared to 40-day means (*Fig 2a-2b*).

Figure 2. *Latitude versus local time plot of 130 day mean (a, a') and 40 day mean (equivalent day, b and b') synthetic zonal and meridional winds, 40 day mean HWM14 zonal (c) and meridional (c') winds, and 40 day mean (equivalent day) cross-track winds (d).*

Latitude vs. Longitude

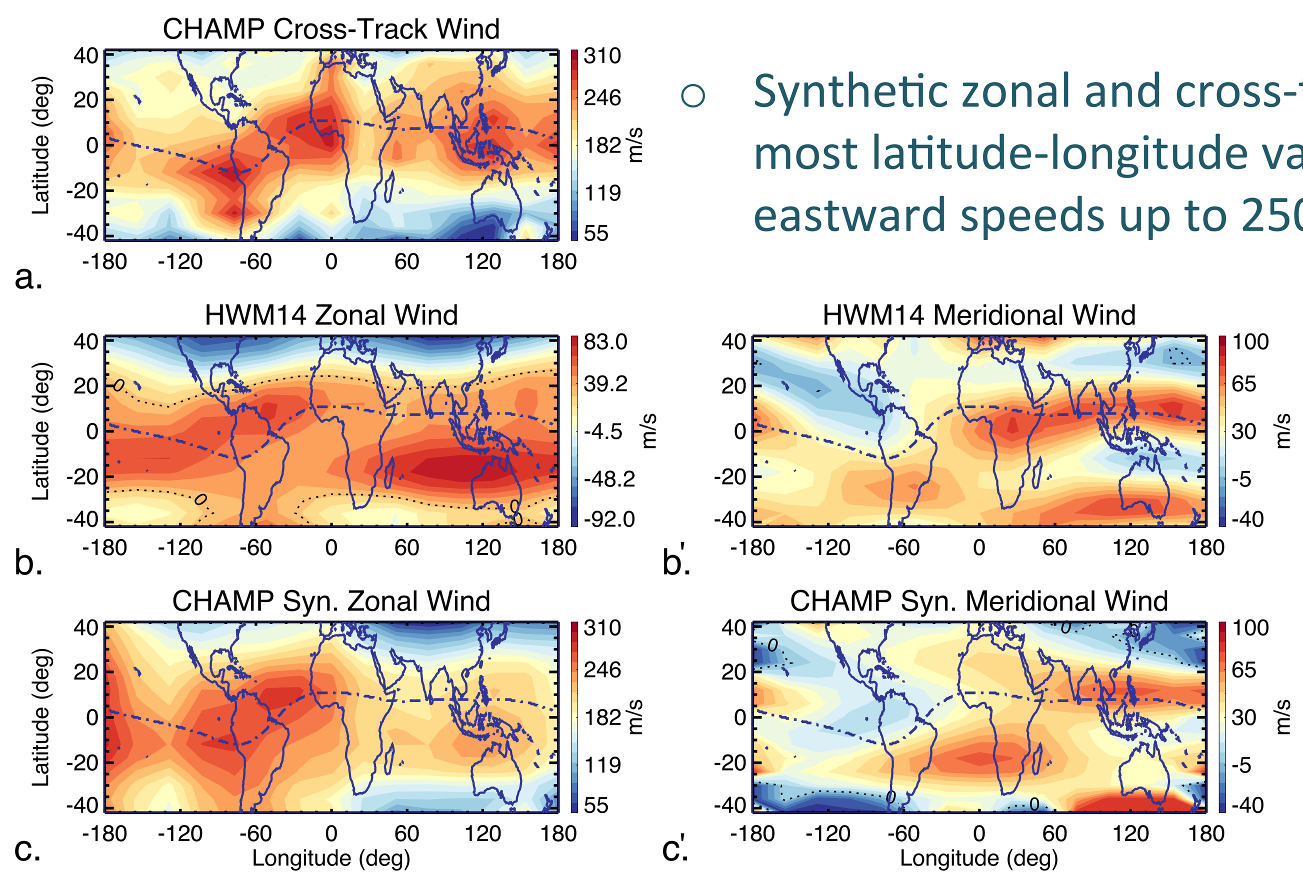

- Synthetic zonal and cross-track winds share most latitude-longitude variability, with large eastward speeds up to 250 m/s (*Fig 3*).
- Zonal winds maximize around geomagnetic equator due to decreased ion drag at 19 LT.
- HWM14 largely underestimates the observed speeds.

Figure 3. *Latitude versus longitude comparisons between (a) CHAMP cross-track wind, (b) HWM14 zonal and(b') meridional winds, and (c) CHAMP synthetic zonal and (c') meridional wind for the 10 day period 12-22 August 2008 at 19 LT.*

Validation

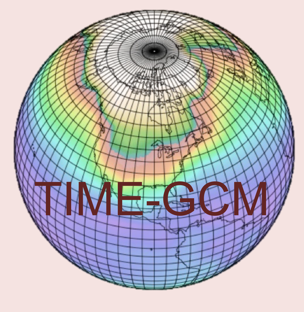

Neutral and electron density from TIME-GCM are converted to pressure gradients and ion drag values, according to *Step 1* and *Step 2*, and used to derive solutions to the momentum equations (*Step 3*).

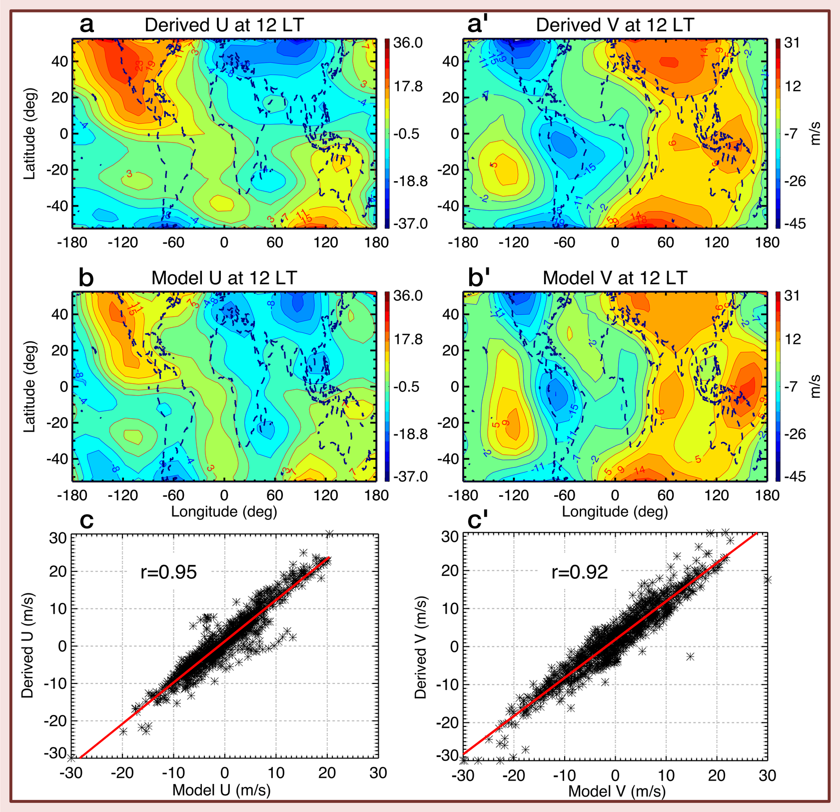

- The ***derived winds capture over 85% of the variability*** in the model winds in latitude vs. longitude (*Fig 4*).
- Similar results are found for different local times and formats.

Figure 4. *Zonal (a-c) and meridional (a'-c') latitude-longitude wind structures at 12 LT from TIME-GCM neutral and electron densities (panels a-a'), self-consistently output from the model (b-b'), and scatter plots (c-c').*

Summary and Conclusions

- CHAMP neutral and electron density are used to infer thermospheric zonal and meridional winds by solving the momentum equations.
- The methodology is validated using TIME-GCM and the **total uncertainty in the synthetic winds is estimated to be ±30%**.
- Synthetic winds are used to highlight the longitude, latitude, local time, and seasonal variability; we found:

1. Strong eastward jet in the postsunset hours around the geomagnetic equator due to decreased ion drag associated with the combined effect of intensified eastward ion drifts due to vertical electric fields and the rapid increase in height of the ionosphere driven by the evening prereversal enhancement of the vertical plasma drift (27 m/s superrotation speeds).
2. The HWM14 empirical model largely underestimates (by over 50%) the latitude, longitude, and local time variability in CHAMP synthetic winds.
3. Significant asymmetry in the latitudinal variation of non-migrating tides are consistent with the presence of higher order modes likely due to the effect of mean winds (result not shown here).
4. Strong seasonal and local time dependency in both zonal and meridional winds (result not shown here).

Associated Journal Article

Gasperini, F., J. M. Forbes, E. N. Doornbos, and S. L. Bruinsma (2016), Synthetic thermosphere winds based on CHAMP neutral and plasma density measurements, J. Geophys. Res. Space Physics, 121, 3699-3721, doi:10.1002/2016JA022392.

References

1. *Bruinsma, S. L., et al. (2004), Atmospheric densities derived from CHAMP/STAR accelerometer observations, Planet. Space Sci., 52, 297-312.*
2. *Challinor, R. A. (1969), Neutral air winds in the ionospheric F-region for an asymmetric global pressure system, Planet. Space Sci., 18, 1485-1487.*
3. *Cooke, D. L., et al. (2003), Ion drift-meter status and calibration, pp. 212–219, Springer, New York.*
4. *Doornbos, E., et al. (2010), Neutral density and crosswind determination* Arbitrarily Oriented Multiaxis Accelerometers on Satellites*, J. Spacecr. Rockets, 47, 580-589.*
5. *Geisler, J. E. (1966), Atmospheric winds in the middle latitude F-region, J. Atmos. Sol. Terr. Phys., 28(8), 703-720.*

Acknowledgements

This work was supported under Grant NNX12AD26G from NASA to the University of Colorado under the U.S. Participating Investigator (USPI) Program for the GOCE Mission